SPhT/96-076

Meanders

P. Di Francesco,

O. Golinelli

and

E. Guitter*,

Service de Physique Théorique, C.E.A. Saclay,
F-91191 Gif sur Yvette, France

Talk given at the conference *The Mathematical Beauty of Physics*, dedicated to the memory of Claude Itzykson, June 5-7 1996, Service de Physique Théorique du C.E.A. Saclay.

07/96

* e-mails: philippe,golinel,guitter@spht.saclay.cea.fr

1. Introduction

The meander problem is one of these apparently very simple problems which resist all attempts to solve them. A fascinating problem which could not go unnoticed with Claude Itzykson. He indeed kept encouraging us at the early stage of this work, even providing us with some mathematical references which were the real starting point of our study. This note is intended as an account of the earlier and latest developments towards a solution of the problem, yet to be invented.

The meander problem is a simply stated combinatorial question: count the number of configurations of a closed non-self-intersecting road crossing an infinite river through a given number of bridges. Despite its apparent simplicity, this problem still awaits a solution, if only for asymptotics when the number of bridges is large. The problem emerged in various contexts ranging from mathematics to computer science [1]. In particular, Arnold re-actualized it in connection with Hilbert's 16th problem, namely the enumeration of ovals of planar algebraic curves [2], and it also appears in the classification of 3-manifolds [3].

Remarkably, the meander problem can be rephrased in the physical language of critical phenomena, through its equivalence with a particular problem of Self-Avoiding Walks: the counting of the compact foldings of a linear chain.

Several techniques have been applied to this problem: direct combinatorial approaches [4] [5], random matrix model techniques [6] [7] [8], an algebraic approach using the Temperley-Lieb algebra and Restricted Solid-On-Solid models [9].

This note is organized as follows. In Sect.2, we define precisely the meander (resp. semi-meander) counting problems, arising in the context of closed (resp. open) chain-folding, and solve them in some simple cases. Sect.3 is an overview of various reformulations of the problem in physical or mathematical terms: the matrix model formulation, which provides us with a complete recursive scheme to compute the meander and semi-meander partition functions, including their higher genus generalizations; the symmetric group formulation, which eventually leads to some compact expressions in terms of the symmetric group characters; the Temperley-Lieb algebra formulation, which gives yet another, completely algebraic viewpoint on the problem. Sect.4 is dedicated to a more direct *enumerative* approach and a thorough analysis of its results in the spirit of critical phenomena. The semi-meander problem is generalized to include the case of several non-intersecting but possibly interlocking roads with a weight q per road, and crossing the river through a total of n bridges. The corresponding generating functions are analyzed as functions

of q, through large n extrapolations, and through their large q asymptotic expansion in powers of $1/q$, for $n \to \infty$. Evidence is given for a phase transition for semi-meanders at a value of $q = q_c \simeq 2$ between a low-q and a large-q regimes, discriminated by the relevance of winding of the roads around the source. The large-q expansion provides an accurate description of the whole $q > q_c$ phase. We gather conclusions and a few conjectures in Sect.5.

2. The meander problem

2.1. Definitions, observables

A *meander* of order n is a planar configuration of a non-self-intersecting loop (road) crossing a line (river), through a given number $2n$ of points (bridges). We consider as equivalent any two configurations which may be continuously deformed into each other, keeping the river fixed (this is therefore a topological equivalence). The number of inequivalent meanders of order n is denoted by M_n. For instance, we have $M_1 = 1$, $M_2 = 2$, $M_3 = 8$... More numbers can be found in [6] [7] [12].

We stumbled on the meander problem by trying to enumerate the distinct *compact folding* configurations of a closed polymer, i.e. the different ways of folding a closed chain of $2n$ identical constituents onto itself. The best image of such a closed polymer is that of a closed strip of $2n$ identical stamps, attached by their edges, serving as hinges in the folding process: a compactly folded configuration of the strip is simply a folded state in which all the stamps are piled up on top of one of them.

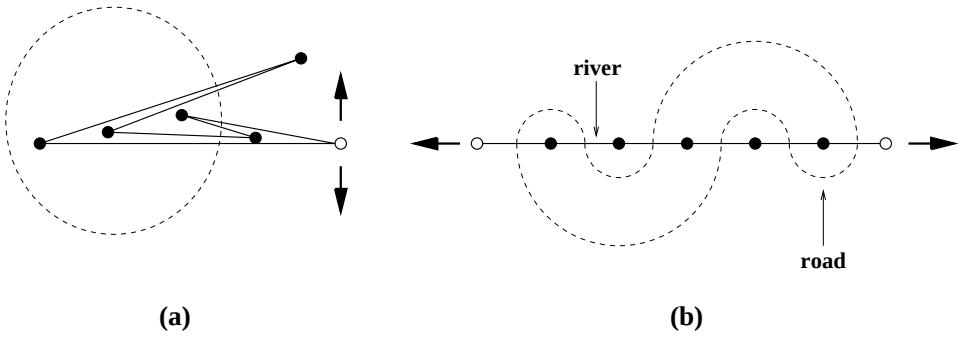

Fig. 1: The mapping between compactly folded closed strip of stamps and meanders. We display a compact folding configuration (a) of a closed strip with $2n = 6$ stamps. To transform it into a meander, first draw a (dotted) line through the centers of the stamps and close it to the left of the picture. Then cut the bottom right hinge (empty circle) and pull its ends apart as indicated by the arrows, so as to form a straight line (b): the straight line forms the river, and the dashed line the road of the resulting meander.

Such a compactly folded configuration is easily identified with a meander configuration as depicted in Fig.1. Draw a closed line (road) passing though the centers (bridges) of all the piled-up monomers, then open one hinge of the polymer (we choose to always open the bottom right one) and pull the stamps apart so as to form a straight line: the latter is identified with the river, whereas the distorted line becomes the road of the resulting meander.

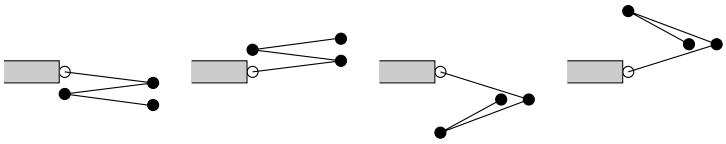

Fig. 2: The 4 inequivalent foldings of a strip of 3 stamps. The fixed stamp is indicated by the empty circle: it is attached to a support (shaded area). The other circles correspond to the edges of the stamps.

When the strip of stamps is open (see Fig.2), we decide to attach the first stamp to a support, preventing the strip from winding around it, while the last stamp has a free extremal edge. In this case, a slightly generalized transformation maps any compactly folded open configuration of $(n-1)$ stamps to what we will call a *semi-meander* configuration of order n, in the following manner.

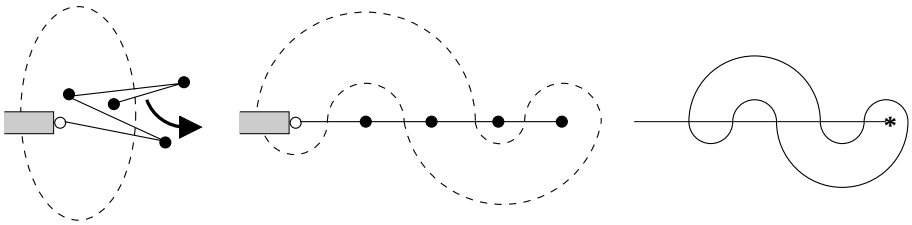

(a) **(b)** **(c)**

Fig. 3: The mapping of a compactly folded configuration of 4 stamps onto a semi-meander of order 5. (a) draw a (dashed) curve through the pile of stamps and the (shaded) support. (b) pull the free edge of the last stamp to form a half-line (the river with a source). (c) the result is a semi-meander configuration of order 5, namely that of a road, crossing a semi-infinite river through 5 bridges (the source of the river, around which the road is free to wind, is indicated by an asterisk).

As shown in Fig.3, draw a curve (road) though the $(n-1)$ centers (bridges) of all the piled-up stamps, then close this curve across the support (this last intersection is the n-th

bridge), and pull the free edge of the last stamp in order to form a straight half-line (river with a source). The resulting picture is a configuration of a road (the curve) crossing a semi-infinite river (stamps and support) through n bridges: this is called a semi-meander configuration of order n. Note that the road in a semi-meander may wind freely around the source of the river, and that consequently the number of bridges may be indifferently even or odd, as opposed to meanders. The number of distinct semi-meanders of order n is denoted by $\bar{M}_n$. For instance, we have $\bar{M}_1 = 1$, $\bar{M}_2 = 1$, $\bar{M}_3 = 2$, $\bar{M}_4 = 4$... More numbers can be found in [4] [7] and in appendix A.

Through its compact folding formulation, the semi-meander problem is a particular reduction of the two-dimensional self-avoiding walk problem, in which only topological constraints are retained. It is therefore natural to define, by analogy with self-avoiding walks the connectivity $\bar{R}$ per stamp and the configuration exponent γ which determine the large n behavior of the semi-meander numbers as follows[1]

$$\bar{M}_n \ \sim \ \bar{c} \ \frac{\bar{R}^n}{n^\gamma} \tag{2.1}$$

The connectivity $\bar{R}$ may be interpreted as the average number of possibilities of adding one stamp to the folded configurations. The exponent γ is characteristic of the (open) boundary condition on the strip of stamps.

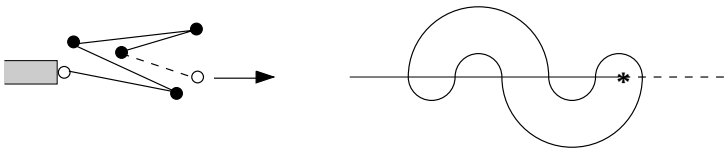

(a) **(b)**

Fig. 4: The "end-to-end distance" of the folded strip of stamps (a) is the number ($w = 1$ here) of stamps to be added to the strip (the added stamp is represented in dashed line), so that the new free end (empty circle) is in contact with the infinity to the right. This coincides with the "winding" of the corresponding semi-meander (b), namely the number of bridges to be added if we continue the river to the right of its source (dashed line).

[1] That the semi-meander numbers $\bar{M}_n$ actually have these leading asymptotics may be proved by deriving upper and lower bounds on $\bar{R}$. See [7] for further details.

A natural observable for self-avoiding walks is the end-to-end distance. The corresponding notion for a compactly folded open strip of stamps is the "distance" between the free end of the strip and, say the support. This distance should also indicate how far the end of the strip is buried inside the folded configuration. It is defined as the minimal length w of a strip of stamps to be attached to the free end, such that a resulting folding with $n-1+w$ stamps has its free end outside of the folding, namely can be connected to the infinity to the right of the folding by a half-line which does not intersect any stamp. Indeed, the infinity to the right can be viewed as the nearest topological neighbor of the support, hence w measures a distance from the free end of the strip to the support. This is illustrated in Fig.4(a), with $n=5$ and $w=1$. In the semi-meander formulation (see Fig.4(b)), this distance w is simply the *winding* of the road around the source of the river, namely the number of bridges to be added if we continue the river to the right of its source. By analogy with self-avoiding walks, we expect the average winding over all the semi-meanders of order n to have the leading behavior

$$\langle w \rangle_n \;\equiv\; \frac{1}{\bar{M}_n} \sum_{\text{semi-meanders}} w \;\sim\; n^{\nu} \tag{2.2}$$

where ν is some positive (end-to-end) exponent $0 \leq \nu \leq 1$, as w is always smaller or equal to n.

In this language, a meander of order n is simply a semi-meander of order $2n$ with winding $w=0$. By analogy with closed (as compared to open) self-avoiding walks, we expect the asymptotics

$$M_n \;\sim\; c\,\frac{R^{2n}}{n^{\alpha}} \tag{2.3}$$

where the connectivity per bridge R is the same as that for semi-meanders (2.1), $R=\bar{R}$, and the configuration exponent $\alpha \neq \gamma$ is characteristic of the closed boundary condition on the strip of stamps.

In the following, we will mainly focus our study on the semi-meander numbers.

2.2. Arches and connected components

Any semi-meander may be viewed as a particular meander by opening the semi-infinite river as indicated by the arrows on Fig.5. In the process, the number of bridges is doubled, hence the order is conserved. The resulting meander however is very peculiar. Note that in general a meander is made of an upper (resp. lower) configuration consisting of non-intersecting arches (arcs of road) connecting the bridges by pairs above (resp. below) the

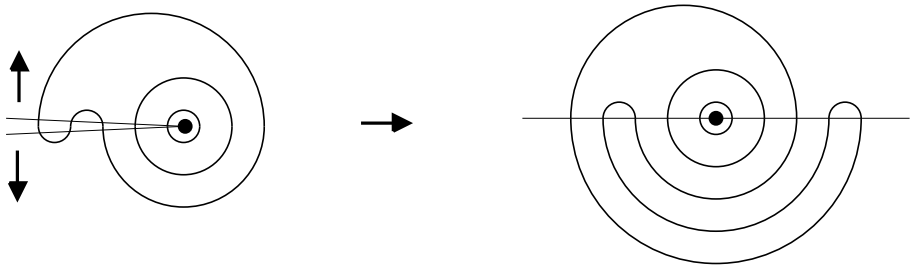

Fig. 5: A semi-meander viewed as a particular meander: the semi-infinite river must be opened up as indicated by the arrows. This doubles the number of bridges in the resulting meander, hence the order is conserved ($n = 5$ here). By construction, the lower arch configuration of the meander is always a rainbow arch configuration of same order.

river. In the present case the lower configuration is fixed: it is called the rainbow arch configuration of order n (the bridge i is connected to the bridge $(2n-i+1)$, $i = 1, 2, ..., n$). On the other hand, the upper arch configuration may take any of the $\bar{M}_n$ values leading to semi-meanders of order n.

There are however

$$c_n \;=\; \frac{(2n)!}{n!(n+1)!} \tag{2.4}$$

distinct arch configurations of order n [7], as is readily proved by recursion ($c_{n+1} = \sum_{0\leq j\leq n} c_j c_{n-j}$, with $c_0 = 1$, hence $c_1 = 1$, $c_2 = 2$, $c_3 = 5$, $c_4 = 14$,...: the c_n are called the Catalan numbers). Hence not all upper arch configurations, once supplemented by a lower rainbow arch configuration of same order, lead to an opened semi-meander ($\bar{M}_n < c_n$). This is because, in general, the corresponding object will have $k \geq 1$ connected components: we call it a semi-meander of order n with k connected components. Indeed, if the river is folded back into a semi-infinite one, we are simply left with a collection of k possibly interlocking semi-meanders of respective orders n_1, n_2,..., n_k, with $n_1 + n_2 + ... + n_k = n$. We always have $1 \leq k \leq n$, and $k = n$ only for the superposition of an upper and a lower rainbow configurations, leading to $2n$ concentric circles in the open river picture. We denote by $\bar{M}_n^{(k)}$ the number of inequivalent semi-meanders of order n with k connected components. In particular, we have $\bar{M}_n^{(1)} = \bar{M}_n$ and $\bar{M}_n^{(n)} = 1$ for all n.

The direct numerical study of the asymptotics of the numbers $\bar{M}_n^{(k)}$ turns out to be delicate, as the natural scaling variable of the problem is the ratio $x = k/n$, which depends on n and takes only a discrete set of values. To circumvent this problem, we will study

the generating function $\bar{m}_n(q)$ for these numbers, also referred to as the *semi-meander polynomial*.

$$\bar{m}_n(q) \;=\; \sum_{k=1}^{n} q^k \;\bar{M}_n^{(k)} \tag{2.5}$$

This quantity makes it possible to study the large n asymptotics of the $\bar{M}_n^{(k)}$ in a global way, by use of extrapolation techniques for all real values of q. The semi-meander polynomial (2.5) may be viewed as the partition function of a statistical assembly of multicomponent semi-meanders of given order n, with a fugacity q per connected component. As such, it is expected to have an extensive large n behavior, namely

$$\bar{m}_n(q) \;\sim\; \bar{c}(q)\;\frac{\bar{R}(q)^n}{n^{\gamma(q)}} \tag{2.6}$$

where $\bar{R}(q)$ is the partition function per bridge, $\gamma(q)$ is a possibly varying exponent and $\bar{c}(q)$ a function independent of n. For $q \to 0$ ($k = 1$), we must recover the connected semi-meanders, namely that $\bar{m}_n(q)/q \to \bar{M}_n$, i.e.

$$\bar{R}(q) \to R \qquad \gamma(q) \to \gamma \qquad \bar{c}(q)/q \to \bar{c} \tag{2.7}$$

(c.f. (2.1)). The notion of winding is well-defined for multi-component semi-meanders as well, as the sum of the individual windings of each connected component, namely the *total* number of times the various roads forming the semi-meander wind around the source of the river. Therefore we define

$$\langle w \rangle_n(q) \;=\; \frac{1}{\bar{m}_n(q)} \sum_{\substack{\text{multicomp.} \\ \text{semi-meanders}}} w\; q^k \sim n^{\nu(q)} \tag{2.8}$$

where $\nu(q)$ is the generalized winding exponent for multi-component semi-meanders, satisfying $0 \leq \nu(q) \leq 1$.

Analogously, we define multi-component meanders of order n, as configurations of k non-intersecting roads ($1 \leq k \leq n$) crossing the river through a total of $2n$ bridges, and denote by $M_n^{(k)}$ their number. We also define the *meander polynomial*

$$m_n(q) \;=\; \sum_{k=1}^{n} q^k \;M_n^{(k)} \tag{2.9}$$

This is nothing but the restriction of (2.5) with $n \to 2n$, to semi-meanders with zero winding $w = 0$. We therefore expect the asymptotics for large n

$$m_n(q) \;\sim\; c(q)\frac{R(q)^{2n}}{n^{\alpha(q)}} \tag{2.10}$$

In this estimate, the partition function per bridge $R(q)$ is expected to be identical to that of semi-meanders $\bar{R}(q)$ only if the winding is irrelevant, namely if $\nu(q)$ is strictly less than 1

$$R(q) \;=\; \bar{R}(q) \quad \text{iff} \quad \nu(q) < 1 \tag{2.11}$$

Otherwise, the fraction of semi-meanders with zero winding may be exponentially small, and we only expect that $R(q) < \bar{R}(q)$ if $\nu(q) = 1$.

2.3. Exact results for large numbers of connected components ($q = \infty$)

For very large q, we simply have

$$\bar{m}_n(q) \;\sim\; q^n \tag{2.12}$$

as the meander polynomial is dominated by the $k = n$ term, corresponding to the unique semi-meander of order n made of n concentric circular roads, each crossing the semi-infinite river only once. The winding of this semi-meander is clearly $w = n$, hence we have, for $q \to \infty$

$$\bar{R}(q) \to q \qquad \gamma(q) \to 0 \qquad \bar{c}(q) \to 1 \qquad \nu(q) \to 1 \tag{2.13}$$

As to meanders, the only way to build a meander of order n with the maximal number n connected components is that each component be a circle, crossing the river exactly twice. This is readily done by taking any upper arch configuration and completing it by reflection symmetry w.r.t. the river. This leads to $M_n^{(n)} = c_n$ (c.f. (2.4)) meanders with n connected components. By Stirling's formula, we find that when $q \to \infty$ the meander polynomial behaves as

$$\begin{aligned} m_n(q) \;&\sim\; c_n \; q^n \\ &\sim\; \frac{1}{\sqrt{\pi}} \frac{(2\sqrt{q})^{2n}}{n^{3/2}} \end{aligned} \tag{2.14}$$

hence, when $q \to \infty$

$$R(q) \to 2\sqrt{q} \qquad \alpha(q) \to 3/2 \qquad c(q) \to 1/\sqrt{\pi} \tag{2.15}$$

This confirms the abovementioned property (2.11) that $R(q) < \bar{R}(q)$ when $\nu(q) = 1$, as $2\sqrt{q} < q$ for large q.

2.4. Exact results for random walks on a half-line ($q = 1$)

When $q = 1$ in (2.5), $\bar{m}_n(1)$ simply counts all the multi-component semi-meanders, irrespectively of their number of connected components. This simplifies the problem drastically, as we are simply left with a purely combinatorial problem which can be solved exactly. The multicomponent semi-meanders are obtained by superimposing any arch configuration of order n with the rainbow of order n, hence

$$\bar{m}_n(1) \;=\; c_n \;\sim \frac{1}{\sqrt{\pi}} \frac{4^n}{n^{3/2}} \tag{2.16}$$

by use of Stirling's formula for large n. This gives the values

$$\bar{R}(1) = 4 \qquad \gamma(1) = 3/2 \qquad \bar{c}(1) = 1/\sqrt{\pi} \tag{2.17}$$

The study of the winding at $q = 1$ is more transparent in the formulation of arch configurations of order n as random walks of $2n$ steps on a semi-infinite line. For each arch configuration of order n, let us label by 1, 2,...,$2n-1$ each segment of river in-between two consecutive bridges, and 0 the leftmost semi-infinite portion, $2n$ the rightmost one. Let $h(i)$, $i = 0, 1, ..., 2n$ denote the number of arches passing at the vertical of the corresponding segment i. By definition, $h(0) = h(2n) = 0$. More generally, going along the river from left to right, we have $h(i) = h(i-1) + 1$ (resp. $h(i) = h(i-1) - 1$) if an arch originates from the bridge i (resp. terminates at the bridge i).

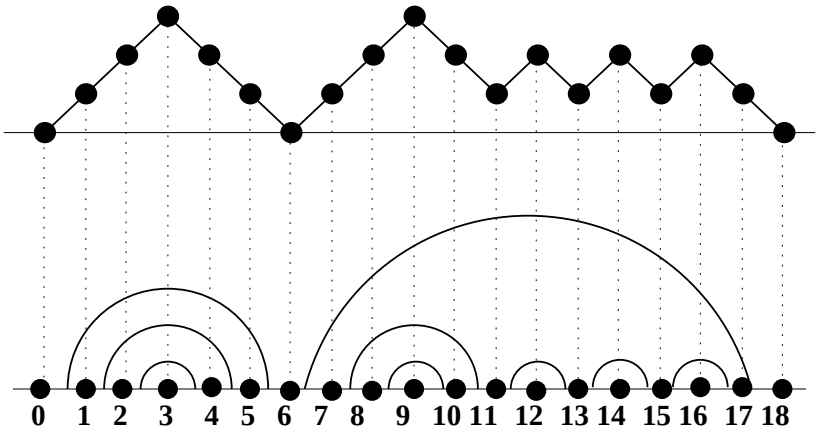

Fig. 6: A walk diagram of 18 steps, and the corresponding arch configuration of order 9. Each dot corresponds to a segment of river. The height on the walk diagram is given by the number of arches intersected by the vertical dotted line.

The function h satisfies $h(i) \geq 0$, for all i, and may be interpreted as a "height" variable, defined on the segments of river, whose graph is nothing but a walk of $2n$ steps as shown in Fig.6. This may be seen as the two-dimensional extent of a brownian motion of $2n$ steps on a half-line, originating and terminating at the origin of the line. This interpretation makes the leading behavior $c_n \sim 2^{2n}$ of (2.16) clear: it corresponds to the 2 possible directions (up or down) that the motion may take at each step. The exponent $3/2$ in (2.16) is characteristic of the boundary condition, namely that the motion is closed and takes place on a half-line (other boundary conditions would lead to different values of γ, e.g. for a closed walk on a line, we would have a behavior $\binom{n}{2n} \sim 2^{2n}/\sqrt{n}$).

In this picture, the winding is simply given by the height $w = h(n)$ of the middle point. Let us evaluate more generally the average height of a point i over the arch configurations of order n. It is given by

$$\langle h(i) \rangle_n \;=\; \frac{1}{c_n} \sum_{h \geq 0} h A_{n,i}(h) \tag{2.18}$$

where $A_{n,i}(h)$ denotes the number of arch configurations of order n such that $h(i) = h$. A simple calculation [9] shows that

$$A_{n,i}(h) \;=\; \left(\binom{i}{\frac{i+h}{2}} - \binom{i}{\frac{i+h}{2}+1} \right) \left(\binom{2n-i}{n-\frac{i-h}{2}} - \binom{2n-i}{n-\frac{i-h}{2}+1} \right) \tag{2.19}$$

as the $A_{n,i}(h)$ walks are simply obtained by gluing two independent walks of i and $2n-i$ steps linking the origin to the height h.

In the case of the winding, $w = h(i = n)$, (2.18) leads to a more compact formula, according to the parity of n

$$\begin{aligned} n = 2p: \qquad \langle w \rangle_{2p} \;&=\; \frac{\binom{2p}{p}^2}{c_{2p}} - 1 \\ n = 2p+1: \qquad \langle w \rangle_{2p+1} \;&=\; 2\frac{\binom{2p}{p}\binom{2p+1}{p}}{c_{2p+1}} - 1 \end{aligned} \tag{2.20}$$

For large n, this gives the following expansion

$$\boxed{\langle w \rangle_n \;=\; 2\sqrt{\frac{n}{\pi}} - 1 + \frac{5}{4\sqrt{\pi n}} + O(1/n^{3/2})} \tag{2.21}$$

irrespectively of the parity of n. This implies that

$$\nu(q=1) \;=\; 1/2 \tag{2.22}$$

This is the well-known result for the Brownian motion, for which the extent of the path scales like $n^{1/2}$ for large n. It is instructive to note that, thanks to (2.21), the observable $w+1$ is less sensitive than w to the finite size effects at $q=1$. This will be useful in the forthcoming numerical estimates for arbitrary q where we observe that the numerical extrapolations are improved by considering $w+1$ instead of w. Using (2.19), we may now compute the probability distribution $P_n(w)$ for an arch configuration of order n to have winding $h(n)=w$, which takes for large n the scaling form

$$P_n(w) \;=\; \frac{1}{c_n} A_{n,n}(w) \;\sim\; \frac{1}{\langle w\rangle_n} f\left(\frac{w}{\langle w\rangle_n}\right) \tag{2.23}$$

with a scaling function f independent of n for large n, readily obtained by use of Stirling's formula, upon writing $w = 2\sqrt{n/\pi}\;\xi$ for large n. This gives

$$\boxed{f(\xi) \;=\; \frac{32}{\pi^2}\xi^2 e^{-\frac{4}{\pi}\xi^2}} \tag{2.24}$$

for all $\xi > 0$.

The meanders of order n are the semi-meanders of order $2n$ with winding $w = h(2n) = 0$. They are therefore built as the juxtaposition of two independent walks of length $2n$. Hence

$$m_n(1) \;=\; (c_n)^2 \;\sim\; \frac{1}{\pi}\frac{4^{2n}}{n^3} \tag{2.25}$$

or, in other words

$$R(1) = \bar{R}(1) = 4 \qquad \alpha(1) = 3 \qquad c(1) = 1/\pi \tag{2.26}$$

This is again in agreement with (2.11), as $\nu(1) = 1/2 < 1$, i.e. the winding is irrelevant at $q=1$.

3. Various formulations of the meander problem

This section is an overview of some very different formulations of the meander problem, each resorting to different mathematical objects (graphs, groups, algebras). The subsequent section will be devoted to yet another approach, dealing with direct enumeration.

3.1. Matrix model

Field theory, as a computational method, involves expansions over graphs weighted by combinatorial factors. In this subsection, we present a particular field theory which precisely generates planar graphs with a direct meander interpretation. The planarity of theses graphs is an important requirement, which ensures that the arches of the meander do not intersect each other, when drawn on a planar surface. The topology of the graphs is best taken into account in matrix models, where the size N of the matrices governs a topological expansion in which the term of order N^{2-2h} corresponds to graphs with genus h. The planar graphs (with $h = 0$) are therefore obtained by taking the large N limit of matrix models (see for instance [14] for a review on random matrices).

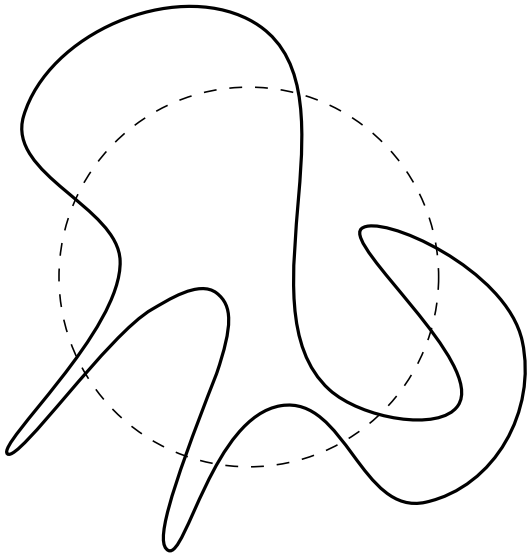

Fig. 7: A sample black and white graph. The white loop is represented in thin dashed line. There are 10 intersections.

The enumeration of (planar) meanders is very close to that of 4–valent (genus 0) graphs made of two self–avoiding loops (say one black and one white), intersecting each other at simple nodes [6]. The white loop stands for the river, closed at infinity. The black loop is the road. Such a graph will be called a black and white graph. An example is given in Fig.7. The fact that the river becomes a loop replaces the order of the bridges by a cyclic order, and identifies the regions above the river and below it. Hence the number of meanders M_n is $2 \times 2n$ (2 for the up/down symmetry and $2n$ for the cyclic symmetry) times that of inequivalent black and white graphs with $2n$ intersections, weighed by the symmetry factor $1/|\mathrm{Aut}(\Gamma)|$ (the inverse of the order of the symmetry group of the graph).

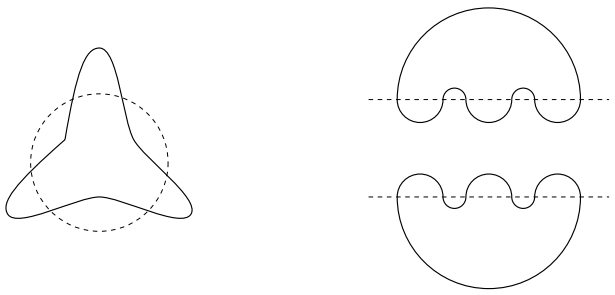

Fig. 8: A particular black and white graph with 6 intersections, and its two associated meanders. The automorphism group of the black and white graph is $\mathbb{Z}_6$.

The same connection holds between $M_n^{(k)}$ and the black and white graphs where the black loop has k connected components.

For illustration, we display a particular black and white graph Γ in Fig.8, together with its two corresponding meanders of order 3. The automorphism group of this black and white graph is $\mathbb{Z}_6$, with order $\mathrm{Aut}(\Gamma) = |\mathbb{Z}_6| = 6$. The two meanders come with an overall factor $1/(2 \times 6)$, hence contribute a total $2 \times 1/12 = 1/6$, which is precisely the desired symmetry factor.

A simple way of generating black and white graphs is the use of the multi–matrix integral (with $m + n$ hermitian matrices of size N denoted by B and W)

$$Z(m, n, c, N) \;=\; \frac{1}{\kappa_N} \int \prod_{\alpha=1}^{m} dB^{(\alpha)} \prod_{\beta=1}^{n} dW^{(\beta)} e^{-N\mathrm{Tr}\; P(B^{(\alpha)}, W^{(\beta)})} \tag{3.1}$$

where the matrix potential reads

$$P(B^{(\alpha)}, W^{(\beta)}) \;=\; \sum_{\alpha} \frac{(B^{(\alpha)})^2}{2} + \sum_{\beta} \frac{(W^{(\beta)})^2}{2} - \frac{c}{2} \sum_{\alpha,\beta} B^{(\alpha)} W^{(\beta)} B^{(\alpha)} W^{(\beta)} \tag{3.2}$$

The measure of integration is the usual Haar measure for hermitian matrices, and the normalization constant κ_N is such that $Z(m, n, c = 0, N) = 1$. In the following, the α and β indices will be referred to as color indices.

The logarithm of the function (3.1) can be evaluated pertubatively as a power series of c. A term of order V in this expansion is readily evaluated as a Gaussian multi–matrix integral. It can be obtained as a sum over 4–valent connected graphs (the logarithm performs the necessary subtractions to go from disconnected to connected graphs), whose

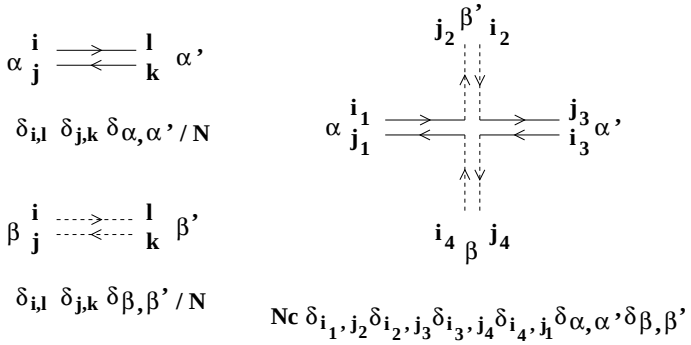

Fig. 9: The Feynman rules for the black and white matrix model. Solid (resp. dashed) double–lines correspond to black (resp. white) matrix elements, whose indices run along the two oriented lines. An extra color index α (resp. β) indicates the number of the matrix in its class, $B^{(\alpha)}$, $\alpha = 1, 2, ..., m$ (resp. $W^{(\beta)}$, $\beta = 1, 2, ..., n$). The only allowed vertices are 4–valent, and have alternating black and white edges: they describe simple intersections of the black and white loops.

V vertices have to be connected by means of the two types of edges

$$\begin{aligned} \text{black edges} \quad \langle [B^{(\alpha)}]_{ij} [B^{(\alpha')}]_{kl} \rangle &= \frac{\delta_{il}\delta_{jk}}{N} \delta_{\alpha\alpha'} \\ \text{white edges} \quad \langle [W^{(\beta)}]_{ij} [W^{(\beta')}]_{kl} \rangle &= \frac{\delta_{il}\delta_{jk}}{N} \delta_{\beta\beta'} \end{aligned} \tag{3.3}$$

which have to alternate around each vertex. The corresponding Feynman rules are summarized in Fig.9. This is an exact realization of the desired connected black and white graphs, except that any number of loops[2] of each color is allowed. In fact, each graph receives a weight

$$N^{2-2h} \; c^V \; m^b \; n^w \tag{3.4}$$

where we have identified the Euler characteristic of the graph as $2 - 2h = V - E + L$ (V vertices with weight N each, E edges with weight $1/N$ each and L loops over which we have to sum the matrix indices, resulting in a weight N each) and b (resp. w) denote the total numbers of black (resp. white) loops.

A simple trick to reduce the number of say white loops w to one is to send the number n of white matrices W to 0, and to retain only the contributions of order 1 in n. Hence

$$f(m, c, N) \;=\; \lim_{n \to 0} \frac{1}{n} \text{Log } Z(m, n, c, N) \;=\; \sum_{\substack{b.\&w. \text{ conn. graphs } \Gamma \\ \text{with one } w \text{ loop}}} N^{2-2h} \; c^V \; m^b \; \frac{1}{|\text{Aut}(\Gamma)|} \tag{3.5}$$

[2] The reader must distinguish between these loops, made of double–lines of a definite color, from the oriented loops along which the matrix indices run.

If we restrict this sum to the leading order N^2, namely the genus 0 contribution ($h = 0$), we finally get a relation to the meander numbers in the form

$$\boxed{\begin{aligned} f_0(m,c) &= \lim_{N\to\infty} \frac{1}{N^2} f(m,c,N) \\ &= \sum_{p=1}^{\infty} \frac{c^{2p}}{4p} \sum_{k=1}^{p} M_p^{(k)} m^k \end{aligned}} \tag{3.6}$$

where the abovementioned relation between the numbers of black and white graphs and multi–component meanders has been used to rewrite the expansion (3.5).

The particular form of the matrix potential (3.2) allows one to perform the exact integration over say all the W matrices (the dependence of P on W is Gaussian), with the result

$$Z(m,n,c,N) = \frac{1}{\theta_N} \int \prod_{\alpha=1}^{m} dB^{(\alpha)} \det\left[\mathbf{I}\otimes\mathbf{I} - c\sum_{\alpha} B^{(\alpha)\ t}\otimes B^{(\alpha)}\right]^{-n/2} e^{-N\mathrm{Tr}\sum_{\alpha}\frac{(B^{(\alpha)})^2}{2}} \tag{3.7}$$

where $\mathbf{I}$ stands for the $N \times N$ identity matrix, $\otimes$ denotes the usual tensor product of matrices, and the superscript t stands for the usual matrix transposition. The prefactor θ_N is fixed by the condition $Z(m,n,c=0,N) = 1$. With this form, it is easy to take the logarithm and to let n tend to 0, with the result

$$\begin{aligned} f(m,c,N) &= -\frac{1}{2\theta_N} \int \prod_{\alpha=1}^{m} dB^{(\alpha)} \mathrm{Tr}\left(\mathrm{Log}\left[\mathbf{I}\otimes\mathbf{I} - c\sum_{\alpha} B^{(\alpha)\ t}\otimes B^{(\alpha)}\right]\right) e^{-N\mathrm{Tr}\sum_{\alpha}\frac{(B^{(\alpha)})^2}{2}} \\ &= \sum_{p=1}^{\infty} \frac{c^p}{2p} \langle \mathrm{Tr}\Big(\sum_{\alpha=1}^{m} B^{(\alpha)\ t}\otimes B^{(\alpha)}\Big)^p \rangle_{\mathrm{Gauss}} \\ &= \sum_{p=1}^{\infty} \frac{c^p}{2p} \sum_{1\le\alpha_1,\ldots,\alpha_p\le m} \langle \left|\mathrm{Tr}(B^{(\alpha_1)}\ldots B^{(\alpha_p)})\right|^2 \rangle_{\mathrm{Gauss}} \end{aligned} \tag{3.8}$$

where we still use the notation $\langle ... \rangle_{\mathrm{Gauss}}$ for the multi–Gaussian average over the matrices $B^{(\alpha)}$, $\alpha = 1, 2, ..., m$. The modulus square simply comes from the hermiticity of the matrices $B^{(\alpha)}$, namely

$$\mathrm{Tr}\Big(\prod B^{(\alpha_i)\ t}\Big) = \mathrm{Tr}\Big(\prod B^{(\alpha_i)\ *}\Big) = \mathrm{Tr}\Big(\prod B^{(\alpha_i)}\Big)^* \tag{3.9}$$

Taking the large N limit (3.6), it is a known fact [14] that correlations should factorize, namely

$$\langle \left| \mathrm{Tr}(\prod_{i=1}^{p} B^{(\alpha_i)}) \right|^2 \rangle_{\mathrm{Gauss}} \underset{N\to\infty}{\longrightarrow} \left| \langle \mathrm{Tr}(\prod_{i=1}^{p} B^{(\alpha_i)}) \rangle_{\mathrm{Gauss}} \right|^2 \tag{3.10}$$

By parity, we see that only even p's give non–vanishing contributions, and comparing with (3.6) we find a closed expression for the meander numbers of order n with k connected components

$$\boxed{\sum_{k=1}^{n} M_n^{(k)} m^k = \sum_{1\le\alpha_1,\ldots,\alpha_{2n}\le m} \left| \lim_{N\to\infty} \langle \frac{1}{N} \mathrm{Tr}(\prod_{i=1}^{2n} B^{(\alpha_i)}) \rangle_{\mathrm{Gauss}} \right|^2} \tag{3.11}$$

This expression is only valid for integer values of m, but as it is a polynomial of degree n in m (with vanishing constant coefficient), the n first values $m = 1, 2, ..., n$ of m determine it completely. So we only have to evaluate the rhs of (3.11) for these values of m to determine all the coefficients $M_n^{(k)}$.

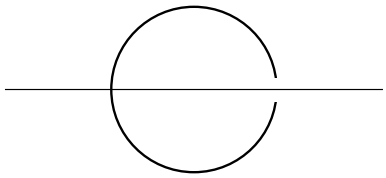

Fig. 10: The connected toric meander of order 1: it has only 1 bridge.

The relation (3.11) suggests to introduce higher genus meander numbers, denoted by $M_p^{(k)}[h]$, with $M_{2n}^{(k)}[0] = M_n^{(k)}$ (note that the indexation is now by the number of intersections, or bridges), through the generating function

$$\boxed{\sum_{h=0}^{\infty} \sum_{k=1}^{\infty} M_p^{(k)}[h] m^k N^{2-2h} = \sum_{1\le\alpha_1,\ldots,\alpha_p\le m} \langle \left| \mathrm{Tr}(\prod_{i=1}^{p} B^{(\alpha_i)}) \right|^2 \rangle_{\mathrm{Gauss}}} \tag{3.12}$$

which incorporates the contribution of all genera in the Gaussian averages. Note that the genus h is that of the corresponding black and white graph and not that of the river or the road alone. In particular, the river (resp. the road) may be contractible or not in

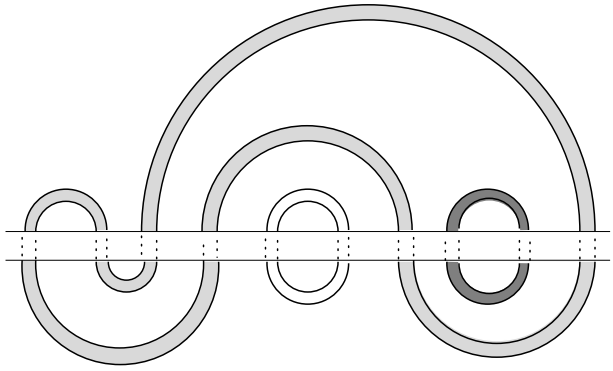

Fig. 11: A typical graph in the computation of the rhs of (3.12). The two p–valent vertices corresponding to the two traces of words are represented as racks of p double legs ($p = 10$ here). The connected components of the resulting meander (of genus $h = 0$ on the example displayed here) correspond to loops of matrices $B^{(\alpha)}$. This is indicated by a different coloring of the various connected components. Summing over all values of α_i yields a factor m per connected component, hence m^3 here.

meanders of genus $h > 0$. As an example the $M_1^{(1)} = 1$ toric meander is represented in Fig.10.

The relation (3.12) can also be proved directly as follows. Its rhs is a sum over correlation functions of the traces of certain words (products of matrices) with themselves. More precisely, using the hermiticity of the matrices $B^{(\alpha)}$, the complex conjugate of the trace $\mathrm{Tr}(\prod_{1\leq i\leq 2n} B^{(\alpha_i)})$ can be rewritten as

$$\mathrm{Tr}(\prod_{1\leq i\leq 2n} B^{(\alpha_i)})^* \;=\; \mathrm{Tr}(\prod_{1\leq i\leq 2n} B^{(\alpha_{2n+1-i})}) \tag{3.13}$$

i.e. in the form of an analogous trace, with the order of the B's reversed. According to the Feynman rules of the previous section in the case of only black matrices, such a correlation can be computed graphically as follows. The two traces correspond to two p–valent vertices, and the Gaussian average is computed by summing over all the graphs obtained by connecting pairs of legs (themselves made of pairs of oriented double–lines) by means of edges. Re–drawing these vertices as small racks of p legs as in Fig.11, we get a sum over all multi–component, multi–genera meanders. More precisely, the edges can only connect two legs with the *same* matrix label α, which can be interpreted as a color: indeed, we have to sum over all colorings of the graph by means of m colors. But this coloring is constrained by the fact that the colors of the legs of the two racks have to be identified two by two (the color of both first legs is α_1,...,of both p-th legs is α_p).

This means that each connected component of the resulting meander is painted with a color $\alpha \in \{1, 2, ..., m\}$. A graph of genus h comes with the usual weight N^{2-2h}. Summing over all the indices $\alpha_1, ..., \alpha_p = 1, 2, ..., m$, we get an extra factor of m for each connected component of the corresponding meander, which proves the relation (3.12).

In the genus 0 case, we must only consider planar graphs, which correspond to genus 0 meanders by the above interpretation. Due to the planarity of the graph, the two racks of $p = 2n$ legs each are connected to themselves through n edges each, and are no longer connected to each other: they form two disjoint arch configurations of order n. This explains the factorization mentioned in eq.(3.10), and shows that the genus 0 meanders are obtained by the superimposition of two arch configurations. The beauty of eq.(3.11) is precisely to keep track of the number of connected components k in this picture, by the m–coloring of the connected components.

This last interpretation leads to a straightforward generalization of (3.12) to semi–meanders, in the form

$$\boxed{\begin{array}{c} \displaystyle\sum_{k=1}^{n} \bar{M}_n^{(k)} m^k \;=\; \sum_{1 \le \alpha_1, ..., \alpha_n \le m} \\ \displaystyle\lim_{N\to\infty} \frac{1}{N} \langle \mathrm{Tr}(B^{(\alpha_1)} B^{(\alpha_2)} ... B^{(\alpha_n)} B^{(\alpha_n)} B^{(\alpha_{n-1})} ... B^{(\alpha_1)}) \rangle_{\mathrm{Gauss}} \end{array}} \tag{3.14}$$

To get this expression, we have used the m–coloring of the matrices to produce the correct rainbow-type connections between the loops of matrices.

All the above expressions for the various meander and semi-meander numbers reduce to the computation of multi-matrix Gaussian averages of traces of words, i.e. of products of matrices. This is readily done by using the so-called loop equations for the Gaussian matrix model (see [7] for all the details), with the following result.

The most general average of trace of word in m matrices in the large N limit is denoted by

$$\begin{array}{l} \gamma^{(m)}_{p_1, p_2, ..., p_{mk}} \;= \\ \displaystyle\lim_{N\to\infty} \frac{1}{N} \langle \mathrm{Tr}\big((B^{(1)})^{p_1} (B^{(2)})^{p_2} ... (B^{(m)})^{p_m} (B^{(1)})^{p_{m+1}} ... (B^{(m)})^{p_{mk}}\big) \rangle_{\mathrm{Gauss}} \end{array} \tag{3.15}$$

In the above, some powers p_j may be zero, but no m consecutive of them vanish (otherwise the word could be reduced by erasing the m corresponding pieces). Of course $2p = \sum_i p_i$

has to be an even number for (3.15) to be non–zero, by parity. For $m = 1$, we easily compute

$$\lim_{N\to\infty} \frac{1}{N}\langle \mathrm{TrB}^p \rangle_{\mathrm{Gauss}} \;=\; \gamma_p^{(1)} \;=\; \begin{cases} c_n & \text{if } p = 2n \\ 0 & \text{otherwise} \end{cases} \tag{3.16}$$

where c_n is the catalan number (2.4). If $\omega = \exp(2i\pi/m)$ denotes the primitive m–th root of unity, then we have the following recursion relation between large N averages of traces of words, for $m \geq 2$

$$\boxed{\gamma^{(m)}_{p_1,p_2,\ldots,p_{mk}} \;=\; -\sum_{j=1}^{mk-1} \omega^j \gamma^{(m)}_{p_1,\ldots,p_j}\ \gamma^{(m)}_{p_{j+1},\ldots,p_{mk}}} \tag{3.17}$$

When j is not a multiple of m, it is understood in the above that the multiplets $(p_1,...,p_j)$ and $(p_{j+1},...,p_{km})$ have to be completed by zeros so a to form sequences of m–uplets. For instance, we write $\gamma_3^{(3)} = \gamma_{3,0,0}^{(3)} = \gamma_{0,0,3}^{(3)}$. Note also that if only $r < m$ matrices are actually used to write a word, the corresponding $\gamma^{(m)}$ can be reduced to a $\gamma^{(r)}$ by erasing the spurious zeros (for instance, $\gamma_{3,0,0}^{(3)} = \gamma_3^{(1)}$). Together with the initial condition $\gamma^{(m)}_{0,\ldots,0,2n+1,0,\ldots,0} = \gamma^{(1)}_{2n+1} = 0$ and $\gamma^{(m)}_{0,\ldots,0,2n,0,\ldots,0} = \gamma^{(1)}_{2n} = c_n$, this gives a compact recursive algorithm to compute all the large N averages of traces of words in any multi–Gaussian matrix model, and henceforth to evaluate the meander and semi-meander numbers.

3.2. Symmetric group

Each arch configuration of order n is naturally labelled by permutation $\mu \in S_{2n}$, the symmetric group over $2n$ objects, in such a way that if we label the bridges of the arch configuration $1, 2, ..., 2n$, the permutation μ indicates the pairs of bridges linked by arches, namely, for any $i = 1, 2, ..., 2n$, $\mu(i)$ is the bridge linked to i by an arch. By definition, μ is made of n cycles of length 2, it is therefore an element of the class $[2^n]$ of S_{2n}. Note that an element of this class generally does not lead to an arch configuration, because the most general pairing of bridges has intersecting arches. A permutation $\mu \in [2^n]$ will be called **admissible** if it leads to an arch configuration.

Let us write the admissibility condition explicitly. This condition states that arches do not intersect each other, namely that the ribbon graph (see Fig.12) with only one $2n$–valent vertex (the $2n$ bridges), whose legs are connected according to the arch configuration, is *planar*, i.e. of genus $h = 0$. This graph has $V = 1$ vertex, and $E = n$ edges (arches). Let

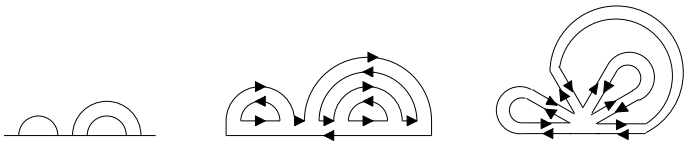

Fig. 12: An arch configuration of order 3 and the corresponding interpretation as a ribbon graph, with $V = 1$ six–valent vertex and $E = 3$ edges. On the intermediate diagram, the arches have been doubled and oriented. These oriented arches indicate the pairing of bridges, i.e. represent the action of μ. Similarly, the oriented horizontal segments indicate the action of the shift permutation σ. Each oriented loop corresponds to a cycle of the permutation $\sigma\mu$.

us compute its number L of oriented loops in terms of the permutation μ. Let σ denote the "shift" cyclic permutation, namely $\sigma(i) = i + 1$, $i = 1, 2, ..., 2n - 1$ and $\sigma(2n) = 1$. Then an oriented loop in the ribbon graph is readily seen to correspond to a *cycle* of the permutation $\sigma\mu$. Indeed, the total number of loops is $L = \text{cycles}(\sigma\mu)$, the number of cycles of the permutation $\sigma\mu$. The admissibility condition reads

$$\begin{aligned} \chi \;&=\; 2 = L - E + V \;=\; 1 - n + \text{cycles}(\sigma\mu) \\ &\Leftrightarrow \quad \text{cycles}(\sigma\mu) \;=\; n + 1 \end{aligned} \tag{3.18}$$

Note that if we demand that the ribbon graph be of genus h, the above condition becomes

$$\text{cycles}(\sigma\mu) \;=\; n + 1 - 2h \tag{3.19}$$

Given an admissible permutation $\mu \in [2^n]$, let us now count the number of connected components of the corresponding semi–meander of order n. Let τ be the "rainbow" permutation $\tau(i) = 2n + 1 - i$. Note that τ changes the parity of the bridge label. On the other hand, the admissible permutation μ is readily seen to also change the parity of the bridge labels. As a consequence, the permutation $\tau\mu$ preserves the parity of bridge labels. In other words, even bridges are never mixed with odd ones. The successive iterations of the permutation $\tau\mu$ describe its cycles. The corresponding meander will be connected iff these cycles are maximal, namely μ has two cycles of length n (one for even bridges, one for odd bridges), i.e. $\tau\mu \in [n^2]$. We get a purely combinatorial expression for connected semi–meander numbers

$$\boxed{\bar{M}_n \;=\; \text{card}\{\mu \in [2^n] \mid \text{cycles}(\sigma\mu) = n + 1, \text{ and } \tau\mu \in [n^2]\}} \tag{3.20}$$

More generally, the semi–meander corresponding to μ will have k connected components iff $\tau\mu$ has exactly k pairs of cycles of equal length (one over even bridges, one over odd ones).

The above conditions on various permutations are best expressed in terms of the characters of the symmetric group. Denoting by $[i^{\nu_i}]$ the class of permutations with ν_i cycles of length i, and labelling the representations of S_{2n} by Young tableaux Y with $2n$ boxes as customary, the characters can be expressed as

$$\chi_Y([i^{\nu_i}]) \;=\; \det\left(p_{i+\ell_i-j}(\theta_.)\right)\Big|_{t_\nu} \;, \tag{3.21}$$

where the Young tableau has ℓ_i boxes in its i-th line, counted from the top, $t_\nu = \prod_i \frac{\theta_i^{\nu_i}}{\nu_i!}$, $p_m(\theta_.)$ is the m-th Schur polynomial of the variables θ_1, θ_2,...

$$p_m(\theta_.) \;=\; \sum_{\substack{k_i\geq 0, i=1,2,\dots \\ \Sigma i k_i = m}} \prod_i \frac{\theta_i^{k_i}}{k_i!} \;, \tag{3.22}$$

and we used the symbol $f(\theta_.)|_{t_\nu}$ for the coefficient of the monomial $\prod_i \frac{\theta_i^{\nu_i}}{\nu_i!}$ in the polynomial $f(\theta_.)$. As group characters, the χ_Y's satisfy the orthogonality relation

$$\sum_Y \chi_Y([\lambda])\chi_Y([\mu]) \;=\; \frac{(2n)!}{|[\lambda]|}\;\delta_{[\lambda],[\mu]} \tag{3.23}$$

where the sum extends over all Young tableaux with $2n$ boxes, $[\lambda]$ denotes the class of a permutation $\lambda \in S_{2n}$, and $|[\lambda]|$ the order of the class. The order of the class $[i^{\nu_i}]$ is simply

$$|[i^{\nu_i}]| \;=\; \frac{(2n)!}{\prod_i i^{\nu_i}\nu_i!} \tag{3.24}$$

The orthogonality relation (3.23) provides us with a means of expressing any condition on classes of permutations in terms of characters. It leads to the following compact expression for the connected semi–meander numbers

$$\begin{aligned}
\bar{M}_n \;&=\; \sum_{\substack{[i^{\lambda_i}]\in S_{2n} \\ \Sigma\lambda_i = n+1}} \sum_{\mu\in[2^n]} \delta_{[\sigma\mu],[i^{\lambda_i}]}\;\delta_{[\tau\mu],[n^2]} \\
&=\; \sum_{\substack{[i^{\lambda_i}]\in S_{2n} \\ \Sigma\lambda_i = n+1}} \sum_{\mu\in S_{2n}} \sum_{Y,Y',Y''} \frac{|[2^n]|\;|[i^{\lambda_i}]|\;|[n^2]|}{((2n)!)^3} \\
&\quad\times \chi_Y([\mu])\chi_Y([2^n])\chi_{Y'}([\sigma\mu])\chi_{Y'}([i^{\lambda_i}])\chi_{Y''}([\tau\mu])\chi_{Y''}([n^2])
\end{aligned} \tag{3.25}$$

Analogous expressions hold for (higher genus) semi–meanders with k connected components and for meanders as well.

3.3. Temperley-Lieb algebra

The Temperley-Lieb algebra of order n and parameter q, denoted by $TL_n(q)$, is defined through its n generators $1, e_1, e_2, ..., e_{n-1}$ subject to the relations

$$\begin{aligned} (i) \qquad e_i^2 &= q\, e_i \quad i = 1, 2, ..., n-1 \\ (ii) \quad [e_i, e_j] &= 0 \quad \text{if } |i-j| > 1 \\ (iii)\ e_i\, e_{i\pm 1}\, e_i &= e_i \quad i = 1, 2, ..., n-1 \end{aligned} \tag{3.26}$$

This definition becomes clear in the "braid" pictorial representation, where the generators act on n parallel strings as follows:

$1 =$ 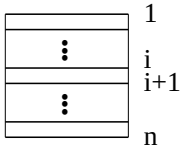

$e_i =$ 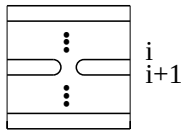

(3.27)

and a product of elements is represented by the juxtaposition of the corresponding braid diagrams, like dominos. The relation (ii) expresses the locality of the e's, namely that the e's commute whenever they involve distant strings. The relations (i) and (iii) read respectively

$(i) \qquad e_i^2 =$ 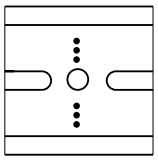

$= q$ 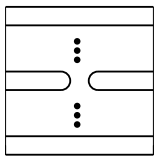

$= q\, e_i$

$(iii)\ e_i\, e_{i+1}\, e_i =$ 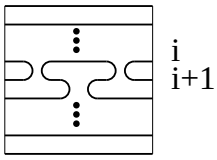

$=$ 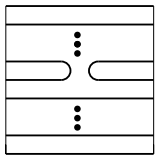

$= e_i$

(3.28)

In the relation (i), the loop has been erased, but affected the weight q. The relation (iii) is simply obtained by stretching the $(i+2)$-th string.

The algebra $TL_n(q)$ is built out of arbitrary products of generators e_i. Up to numerical factors depending on q, any such product can be reduced by using the relations (i)-(iii). The algebra $TL_n(q)$, as a real vector space, is therefore naturally endowed with the basis formed by all the distinct reduced elements of the algebra. For illustration, the reduced elements of $TL_3(q)$ read

$1 =$ 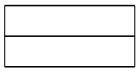
$e_1 =$ 
$e_2 =$ 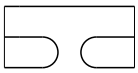
$e_1 e_2 =$ 
$e_2 e_1 =$ 

(3.29)

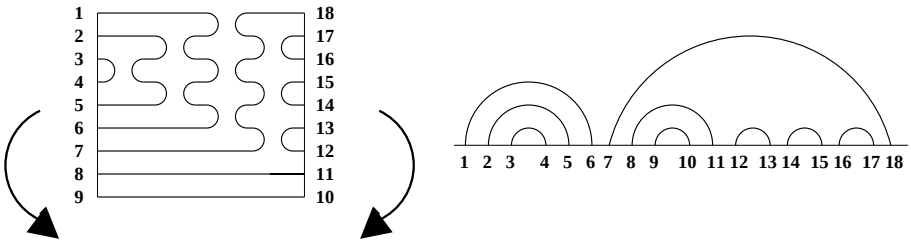

Fig. 13: The transformation of a reduced element of $TL_9(q)$ into an arch configuration of order 9. The reduced element reads $e_3e_4e_2e_5e_3e_1e_6e_4e_2$.

Let us now show that the reduced elements of $TL_n(q)$ are in one to one correspondence with arch configurations of order n. This is most clearly seen by considering the braid pictorial representation of a reduced element. Such a diagram has no internal loop (by virtue of (i)), and all its strings are stretched (using (iii)). As shown in Fig.13, one can construct a unique arch configuration of order n by deforming the diagram so as to bring the $(2n)$ ends of the strings on a line. This deformation is invertible, and we conclude that, as a vector space, $TL_n(q)$ has dimension

$$\dim(TL_n(q)) \;=\; c_n \tag{3.30}$$

This identification allows us to denote the elements of the basis of reduced elements of $TL_n(q)$ by the corresponding arch configurations a of order n.

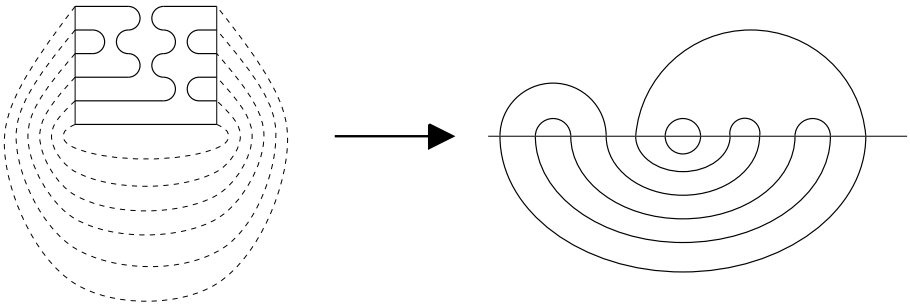

Fig. 14: The trace of an element $e \in TL_6(q)$ is obtained by identifying the left and right ends of its strings (dashed lines). In the arch configuration picture, this amounts to closing the upper configuration by a rainbow of order 6. The corresponding semi-meander has 3 connected components, hence $\mathrm{Tr}(e) = q^3$.

A scalar product on $TL_n(q)$ is defined as follows. First one introduces a trace over $TL_n(q)$. From the relation (i) of (3.26), we see that in any element of $TL_n(q)$ each closed

loop may be erased and replaced by a prefactor q. Taking the trace of a reduced basis element a corresponds to identifying the left and right ends of each string as in Fig.14, and assigning an analogous factor to each closed loop, which results in a factor

$$\mathrm{Tr}(a) \;=\; q^{c(a)} \tag{3.31}$$

where $c(a)$ is precisely the number of connected components of the closure of a by a rainbow of order n: indeed, the rainbow connects the i-th bridge to the $(2n+1-i)$-th, which exactly corresponds to the above identification of string ends. This makes the connection with meander problems clear. In particular, this permits to identify the semi-meander polynomial as

$$\bar{m}_n(q) \;=\; \sum_{\text{arch configs. } a} q^{c(a)} \;=\; \mathrm{Tr}\Big(\sum_{\text{red. basis}} a\Big) \tag{3.32}$$

We also define the transposition on $TL_n(q)$, by its action on the generators $e_i^t = e_i$, and the relation $(ab)^t = b^t a^t$ for any $a, b \in TL_n(q)$. In the arch configuration picture, this corresponds to the reflection $i \to (2n+1-i)$ of the bridges. It may also be viewed as the reflection w.r.t. the river.

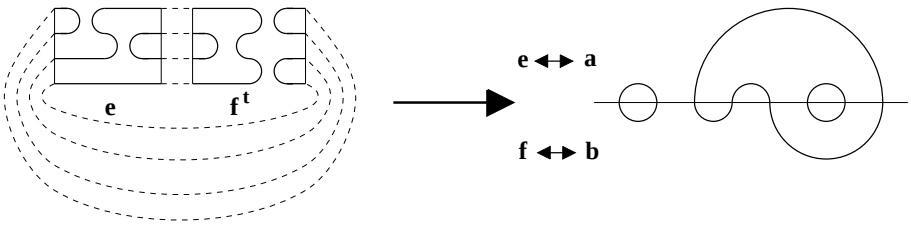

Fig. 15: The scalar product (e, f) is obtained by first multiplying e with f^t, and then identifying the left and right ends of the strings (by the dashed lines). Here we have $(e, f) = q^3$. The corresponding meander is obtained by superimposition of the upper arch configuration a corresponding to e and lower arch configuration b corresponding to f (the transposition of f is crucial to recover b as lower arch configuration). Here the meander has $c(a, b) = c(e, f) = 3$ connected components.

For any two elements e and $f \in TL_n(q)$, the scalar product is defined as

$$(e, f) \;=\; \mathrm{Tr}(e\, f^t) \tag{3.33}$$

This has a simple interpretation in terms of meanders. We have indeed

$$(e, f) \;=\; q^{c(e,f)} \;=\; q^{c(a,b)} \tag{3.34}$$

where $c(e,f) = c(a,b)$ is the number of connected components of the meander obtained by superimposing the a and b arch configurations corresponding respectively to e and f (see Fig.15 for an example).

The Gram matrix $\mathcal{G}_n(q)$ of the reduced basis of $TL_n(q)$ is the $c_n \times c_n$ symmetric matrix with entries equal to the scalar products of the basis elements, namely

$$\boxed{\left[\mathcal{G}_n(q)\right]_{a,b} \;=\; \mathrm{Tr}(ab^t) \;=\; q^{c(a,b)}} \tag{3.35}$$

For instance, $\mathcal{G}_3(q)$ reads, in the basis (3.29), with the order $(e_2e_1, e_1e_2, e_2, e_1, 1)$:

$$\mathcal{G}_3(q) \;=\; \begin{pmatrix} q^3 & q^2 & q^2 & q & q^2 \\ q^2 & q^3 & q & q^2 & q \\ q^2 & q & q^3 & q^2 & q \\ q & q^2 & q^2 & q^3 & q^2 \\ q^2 & q & q & q^2 & q^3 \end{pmatrix} \tag{3.36}$$

The meander and semi-meander polynomials are easily expressed in terms of the Gram matrix. Arranging the elements of basis 1 by growing winding (in particular, the unit 1 is the last element), and defining the c_n-dimensional vectors

$$\vec{u} \;=\; (1,1,1,\cdots,1) \qquad \vec{v} \;=\; (0,0,\cdots,0,1) \tag{3.37}$$

we have

$$\begin{aligned} m_n(q) &= \vec{u}\cdot\mathcal{G}_n(q)\vec{u} \\ \bar{m}_n(q) &= \vec{v}\cdot\mathcal{G}_n(q)\vec{u} \end{aligned} \tag{3.38}$$

where $\vec{x}\cdot\vec{y}$ denotes the ordinary Euclidian scalar product of $\mathbb{R}^{c_n}$. Moreover, we also have

$$m_n(q^2) \;=\; \mathrm{tr}\big(\mathcal{G}_n(q)^2\big) \tag{3.39}$$

The Gram matrix $\mathcal{G}_n(q)$ contains therefore all the information we need about meanders and semi-meanders. In [10], using the representation theory of the Temperley-Lieb algebra [15], we have computed exactly the determinant of the Gram matrix (3.35), with the simple result

$$\boxed{\begin{aligned} D_n(q) &= \det\big(\mathcal{G}_n(q)\big) \;=\; \prod_{i=1}^{n} U_i(q)^{a_{n,i}} \\ a_{n,i} &= \binom{2n}{n-i} - 2\binom{2n}{n-i-1} + \binom{2n}{n-i-2} \end{aligned}} \tag{3.40}$$

where $U_i(q)$ are the Chebishev polynomials of the second kind ($U_j(x) = xU_{j-1}(x) - U_{j-2}(x)$, $U_0(x) = 1$, $U_1(x) = x$). We have also used the convention that $\binom{j}{k} = 0$ if $j < 0$. For instance, the determinant of the matrix $\mathcal{G}_3(q)$ (3.36) reads

$$D_3(q) \;=\; U_1(q)^4\, U_2(q)^4\, U_3(q) \;=\; q^5\,(q^2-1)^4\,(q^2-2) \tag{3.41}$$

A remarkable fact is that $D_n(q)$ has only real zeros z, with $|z| < 2$. Actually, the representation theory of $TL_n(q)$ enables one to orthogonalize the Gram matrix (3.35) explicitly. This in turn translates into new "RSOS-type" expressions for the semi-meander and meander polynomials through (3.38) and (3.39) (see [10] for details). These expressions display drastic differences according to whether $|q|$ is larger or smaller than 2, a critical value which will re-emerge in the subsequent section. Hopefully these will enable one to study the large n asymptotics of the corresponding polynomials.

4. Exact enumeration and its analyses: the winding transition

In this section, we present results of an exact enumeration of $\bar{M}_n^{(k)}$ for small n ($n \leq 29$), and analyze their large n extrapolation. The enumeration is performed by implementing on a computer a recursive algorithm which describes all the semi-meanders up to some given order. Clearly, the complexity is proportional to the Catalan numbers ($c_n \sim 4^n$) hence the limitation on n.

This data is then used to derive a large q expansion of the semi-meander polynomial large n asymptotics, thanks to some remarkable property of the semi-meander numbers with large number of connected components.

The main result of this study is a strong evidence for a winding transition from a low-$q < q_c$ phase of irrelevant winding to a large-$q > q_c$ phase of relevant winding for semi-meanders.

4.1. The main recursion relation

We derive now a recursion relation generating all the semi-meanders of order $(n+1)$ from those of order n.

We start from any semi-meander of order n with k connected components, in the open-river picture. We may construct a semi-meander of order $(n+1)$ in either following way (denoted (I) or (II)), as illustrated in Fig.16

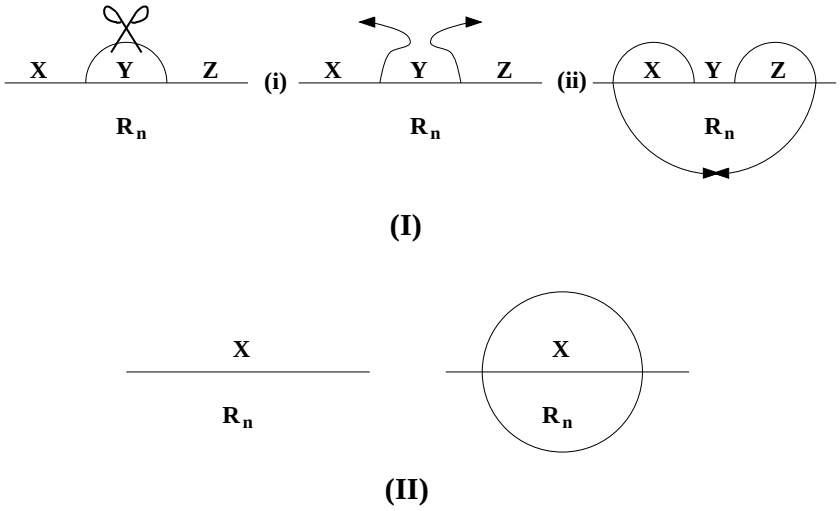

Fig. 16: The construction of all the semi–meanders of order $n+1$ with arbitrary number of connected components from those of order n. Process (I): (i) pick any exterior arch and cut it (ii) pull its edges around the semi–meander and paste them below. The lower part becomes the rainbow configuration $\mathcal{R}_{n+1}$ of order $n+1$. This process preserves the number of connected components $k \to k$. Process (II): draw a circle around the semi–meander of order n. This process adds one connected component $k \to k+1$.

(I) Pick any exterior arch, i.e. any arch with no other arch passing above it. Cut it and pull its ends all the way around the others (in order to add two bridges), and reconnect them below, by creating an extra concentric lower arch for the rainbow. In this process, we have $n \to n+1$, but the number of connected components has not changed: $k \to k$. Another way of picturing this transformation is the following: one simply has pulled the exterior arch all the way around the semi-meander and brought it below the figure, creating two new bridges along the way. As no cutting nor pasting is involved, the number of connected components is clearly preserved.

(II) Draw a circle around the semi-meander. This adds a lower concentric semi-circle which increases the order of the rainbow to $(n+1)$, and also adds one connected component to the initial semi-meander $k \to k+1$.

These two possibilities exhaust all the semi-meanders of order $(n+1)$, as the transformation is clearly invertible, by pulling back up the lower external arch of the rainbow. Note that by construction, there are as many possibilities for the process (I) as exterior arches, and the transformation is therefore one-to-many.

We may now construct a tree of all the semi-meanders, generated recursively from that of order 1 (root), as displayed in Fig.17. Note that we have adopted the open-river formulation to represent them.

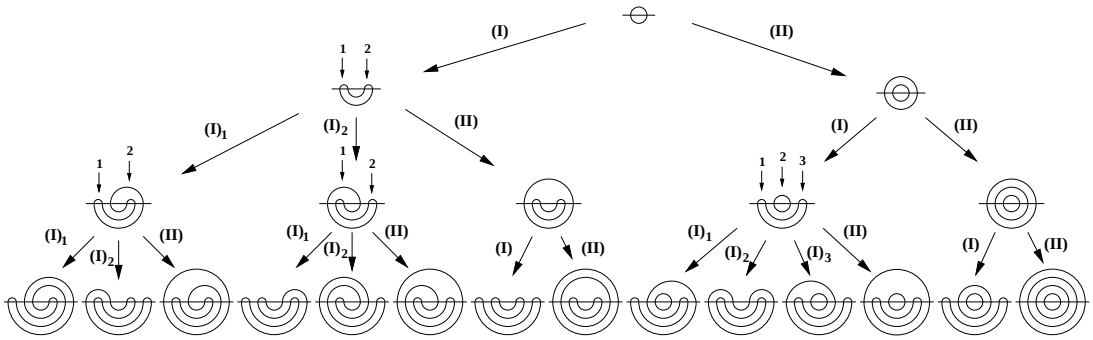

Fig. 17: The tree of semi-meanders down to order $n = 4$. This tree is constructed by repeated applications of the processes (I) and (II) on the semi-meander of order 1 (root). We have indicated by small vertical arrows the multiple choices for the process (I), each of which is indexed by its number. The number of connected components of a given semi-meander is equal to the number of processes (II) in the path going from the root to it, plus one (that of the root).

Keeping track of the connected components, this translates into the following relation between the semi-meander polynomials

$$\bar{m}_{n+1}(q) \;=\; \bar{m}_n(q)\langle \text{ext.arch.}\rangle_n(q) + q\bar{m}_n(q) \tag{4.1}$$

where we denoted by $\langle \text{ext.arch.}\rangle_n(q)$ the average number of exterior arches in a semi-meander of order n, weighed by q^k, k its number of connected components. In (4.1), the first term corresponds to all the processes (I), whereas the second term corresponds to (II).

Taking the large n limit in (4.1), this permits to interpret

$$\bar{R}(q) - q \;=\; \langle \text{ext.arch.}\rangle_\infty(q) \tag{4.2}$$

as the limit when $n \to \infty$ of the average number of exterior arches in semi-meanders of order n, weighed by an activity q per connected component. For large q, we get the limit

$$\bar{R}(q) - q \;\to\; 1 \tag{4.3}$$

as the corresponding leading semi-meander has only one exterior arch. We also find for $q = 1$ that there is an average of $3 = 4 - 1$ exterior arches in arbitrary arch configurations of order n. Finally, for $q = 0$, the partition function per bridge $\bar{R}(0)$ is interpreted as the average number of exterior arches in connected semi-meanders.

4.2. Numerical analysis

By implementing the above recursion on a computer, we have been able to enumerate the semi-meander numbers up to $n = 29$ bridges, and the expectation values of various observables up to $n = 24$ bridges. Many of these results can be found in [7] [10]. For illustration, we give below a typical Fortran program, usable on any computer, for the enumeration of the connected semi-meanders.

```
      PARAMETER (nmax = 14)                    ! maximal order
      INTEGER A(-nmax+1:nmax)                  ! arch representation
      INTEGER Sm(nmax)                         ! semi-meander counter
      INTEGER n                                ! current depth (or order)
      INTEGER j                                ! next branch to visit
      DATA n, Sm /0, nmax*0/                   ! n and Sm initialized to 0
      A(0) = 1                                 ! single-arch semi-meander
      A(1) = 0
2     n = n + 1                                ! a new node is visited
      Sm(n) = Sm(n) + 1
      j = -n + 1                               ! leftmost (exterior) arch
1     IF((n.EQ.nmax).OR.(j.EQ.n+1)) GOTO 3     ! up or down ?
      A(A(j)) = n+1                            ! go down with process (I)
      A(n+1) = A(j)
      A(j) = -n
      A(-n) = j
      GOTO 2
3     A(A(-n+1)) = A(n)                        ! going up
      A(A(n)) = A(-n+1)
      j = A(n)+1                               ! next arch to break
      n = n - 1
      IF (n .GT. 1) GOTO 1
      PRINT '(i3, i15)', (n, Sm(n), n = 1, nmax)
      END
```

This program lists the numbers $Sm(n) = \bar{M}_n$ for $n = 1, ..., nmax$.

This data was further analyzed by large n extrapolation, and we now present a few results.

The results for $\bar{R}(q)$ and $R(q)$ are displayed in Fig.18. The two functions are found to coincide in the range $0 \leq q \leq q_c$ with $q_c \simeq 2$, and to split into $\bar{R}(q) > R(q)$ for $q > q_c$. As explained before, the comparison between $\bar{R}(q)$ and $R(q)$ determines directly whether $\nu(q)$ is 1 or not. The result of Fig.18 is therefore the signal of a phase transition at $q = q_c$ between a low-q regime where the winding is essentially irrelevant ($\nu(q) < 1$) and a large-q phase with relevant winding ($\nu(q) = 1$).

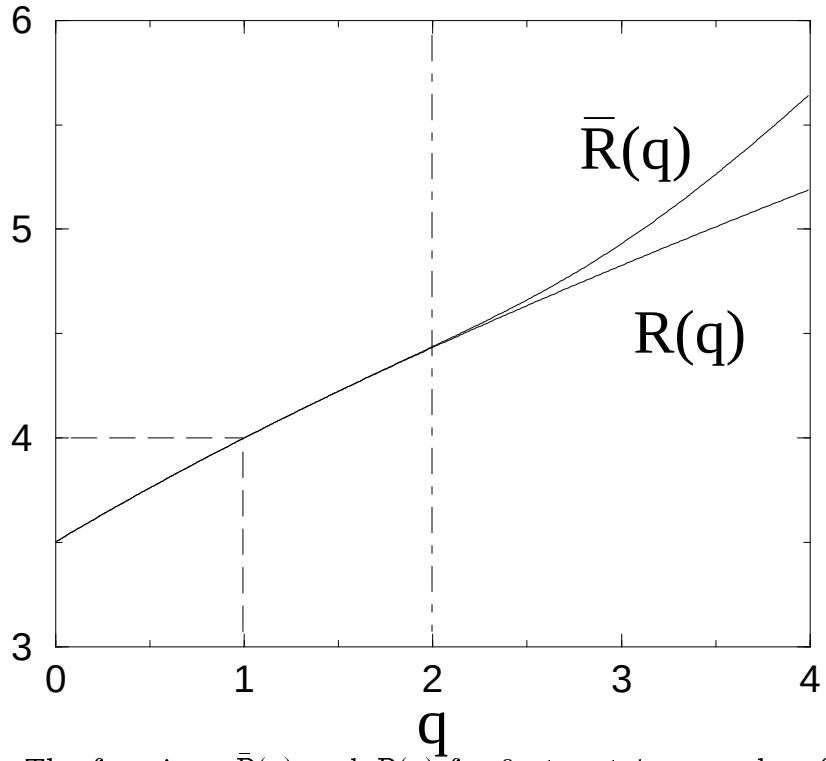

Fig. 18: The functions $\bar{R}(q)$ and $R(q)$ for $0 \leq q \leq 4$ as results of large n extrapolations. The two curves coincide for $0 \leq q \leq 2$ and split for $q > 2$ with $\bar{R}(q) > R(q)$. Apart from the exact value $\bar{R}(1) = R(1) = 4$, we find the estimates $\bar{R}(0) = 3.50(1)$, $\bar{R}(2) = 4.44(1)$, $\bar{R}(3) = 4.93(1)$ and $\bar{R}(4) = 5.65(1)$.

This is compatible with the direct extrapolation for $\nu(q)$ displayed in Fig.19, which is however less reliable in the region around $q = 2$, due to its sub-leading (and probably discontinuous) character.

The configuration exponent for semi-meanders $\gamma(q)$ is represented in Fig.20, for two different orders in our extrapolation scheme. The extrapolation proves to be stable for $0 < q < 2$. For $q > 2$, it develops oscillations around a mean value, estimated to vanish ($\gamma(q) \sim 0$) for q large enough.

By analogy with critical phenomena, in addition to the scaling behaviors (2.6), (2.10) and (2.8) involving the critical exponents $\gamma(q)$, $\alpha(q)$ and $\nu(q)$, we expect to find more refined scaling laws involving scaling functions. A particular example of such scaling functions has been derived for $q = 1$ (2.23), for the probability distribution $P_n(w)$ of the winding w among arch configurations of order n. It involves the scaling function (2.24). For $q = 0$ we expect the same behavior for the corresponding probability distribution

$$P_n^{(0)}(w) \;=\; \frac{\bar{M}_n^{(1)}(w)}{\bar{M}_n^{(1)}} \tag{4.4}$$

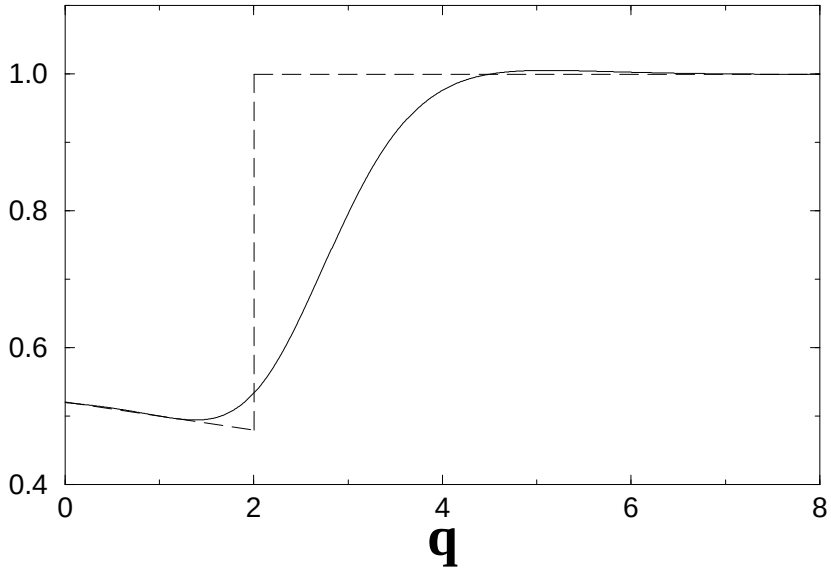

Fig. 19: The winding exponent $\nu(q)$ for $0 \leq q \leq 8$, as obtained from a large n extrapolation. We observe a drastic change of behavior between low q's and large q's, with an intermediate regime where the extrapolation fails, hence is not reliable. The dashed line indicates a possible scenario for the exact function $\nu(q)$, compatible with a transition at $q_c \simeq 2$. Apart from the exact value $\nu(1) = 1/2$, we read $\nu(0) = 0.52(1)$.

of winding w among connected semi-meanders of order n. We expect the scaling behavior

$$P_n^{(0)}(w) \;\sim\; \frac{1}{\langle w \rangle_n(0)} f^{(0)}\left(\frac{w}{\langle w \rangle_n(0)}\right) \tag{4.5}$$

This is precisely what we observe in Fig.21, where we plot $\langle w+1 \rangle_n(0)\, P_n^{(0)}(w)$ as a function of the reduced variable $\xi = (w+1)/\langle w+1 \rangle_n(0)$ for different values of n. Indeed, as already explained in the $q = 1$ case, we have taken the variable $(w+1)$ instead of w to improve the convergence. All the data accumulate on a smooth curve, which represents the scaling function $f^{(0)}(\xi)$. The shape of this function is reminiscent of that of the end-to-end distribution for polymers. By analogy, we expect a certain power law behavior for small ξ

$$f^{(0)}(\xi) \;\sim\; \xi^{\theta} \tag{4.6}$$

where θ satisfies the relation

$$\alpha - \gamma \;=\; \nu(1+\theta) \tag{4.7}$$

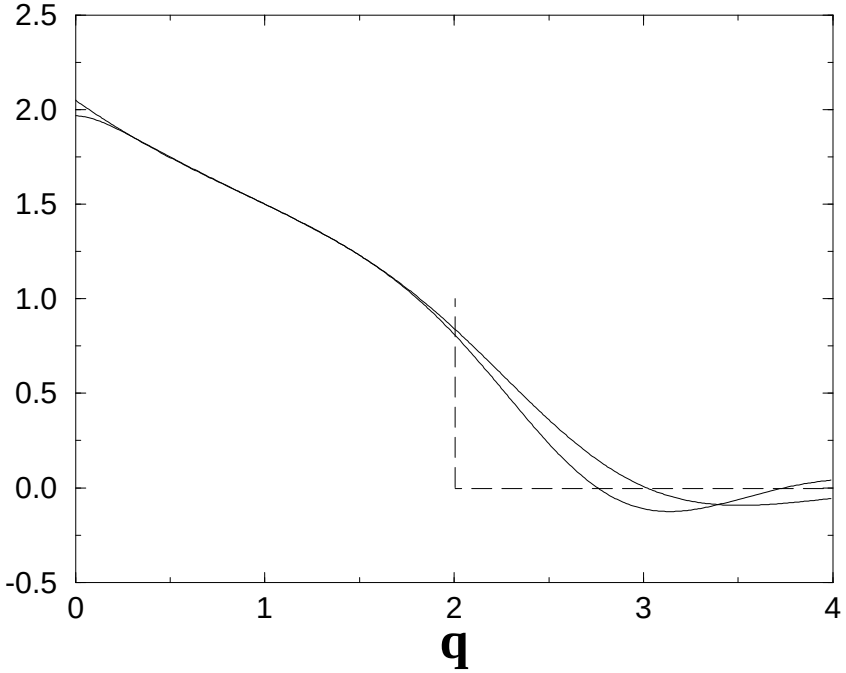

Fig. 20: The configuration exponent $\gamma(q)$ for $0 \leq q \leq 4$, from two different large n extrapolations. Apart from the exact value $\gamma(1) = 3/2$, we estimate $\gamma(0) \simeq 2$.

obtained by identifying

$$P_{2n}^{(0)}(0) \;\propto\; \frac{1}{n^\nu} f^{(0)}\left(\frac{1}{n^\nu}\right) \tag{4.8}$$

to

$$\frac{\bar{M}_{2n}^{(1)}(0)}{\bar{M}_{2n}^{(1)}} \;=\; \frac{M_n}{\bar{M}_{2n}} \propto n^{\gamma-\alpha} \tag{4.9}$$

For large ξ, we expect a behavior $f^{(0)}(\xi) \sim \exp(-\text{const.}\,\xi^\delta)$ with a possible Fisher-law behavior $\delta = 1/(1-\nu)$. The observed function of Fig.21 is compatible with these limiting behaviors, although we cannot extract reliable estimates of the exponents θ and δ.

4.3. Large q asymptotic expansions

In the previous subsection, we have observed two regimes for the semi-meander polynomials, namely a low-q regime in which the winding is irrelevant and a large-q regime where the winding is relevant, separated by a transition at a value of $q = q_c \simeq 2$. On the other hand, we have already exhibited an exact solution of the problem at $q = \infty$ (2.13), and a first correction thereof for large q in (4.3). It is therefore tempting to analyze the large q phase by a systematic expansion in $1/q$.

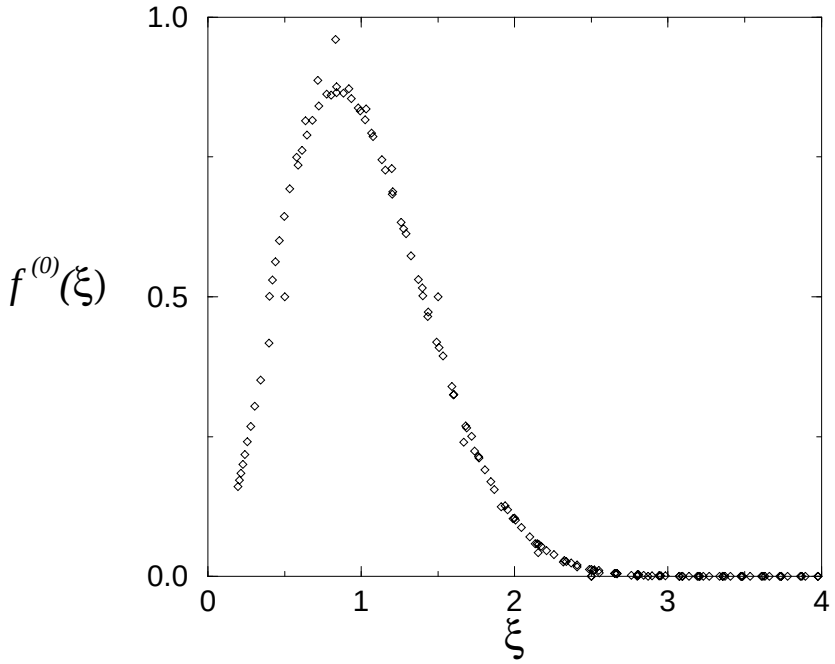

Fig. 21: Plot of $\langle w+1\rangle_n(0)\, P_n^{(0)}(w)$ as a function of the reduced variable $\xi = (w+1)/\langle w+1\rangle_n(0)$ for $n = 2, 3, ..., 24$. The points accumulate to a smooth scaling function $f^{(0)}(\xi)$. The erratic points correspond to small values of n, which have not reached the asymptotic regime.

Let us write the large q expansion of the semi-meander polynomial $\bar{m}_n(q)$ of eq.(2.5) as

$$\bar{m}_n(q) \;=\; q^n \;(\bar{M}_n^{(n)} + \frac{\bar{M}_n^{(n-1)}}{q} + \frac{\bar{M}_n^{(n-2)}}{q^2} + \cdots) \tag{4.10}$$

involving the semi-meander numbers in the form $\bar{M}_n^{(n-k)}$, $k = 0, 1, 2, ...$ Remarkably, these numbers display some polynomial structure.

When $k = 0$, there is a unique semi-meander of order n with n connected components, namely that made of n concentric circular roads, each intersecting the river through one bridge, and therefore winding once around the source. Hence we identify the first polynomial p_0 of degree 0 as

$$p_0(n) \;=\; \bar{M}_n^{(n)} \;=\; 1 \tag{4.11}$$

When $k = 1$, all semi-meanders of order n with $n-1$ connected components are made of $n-2$ concentric circles intersecting the river once each, plus one loop, drawn in-between two consecutive circles, which intersects the river through two bridges and has no winding. There are $n-1$ available positions for this extra loop, resulting in

$$p_1(n) \;=\; \bar{M}_n^{(n-1)} \;=\; n-1 \tag{4.12}$$

where we have identified the result as a polynomial p_1 of degree 1 in n.

More generally, using the recursive construction of the previous section, one can prove the following proposition: the number $\bar{M}_n^{(n-k)}$ is equal to a polynomial $p_k(n)$ of degree k in n, for all $k \geq 0$ and $n \geq 2k-1$. The proof is purely combinatorial, and to just give a flavor of it let us compute the leading coefficient of $p_k(n)$. The $\bar{M}_n^{(n-k)}$ semi-meanders of order n with $n-k$ components are generated in the tree 17, starting from the root, by exactly k applications of the process (I) and $n-1-k$ applications of the process (II). This leads to $\binom{n-1}{k} \sim n^k/k! \sim p_k(n)$ possible choices for $n >> k$. The choices are however not independent, as consecutive applications of the process (I) may lead to more possibilities. Those are included in the lower order coefficients of $p_k(n)$, gathering lower order combinatorial factors. When $n \leq 2k-2$, some non-polynomial corrections emerge, signaling the break-down of the large q phase of semi-meanders. In the latter, the polynomial $\bar{m}_n(q)$ is asymptotic to the series

$$q^n \sum_{k=0}^{\infty} p_k(n) q^{-k} \tag{4.13}$$

which must display an asymptotic behavior of the form (2.6). This induces strong constraints on the polynomials $p_k(n)$, which allow for their complete determination up to $k=18$, out of their first values for small n, which were enumerated exactly up to $n=27$ (the polynomials p_k are listed in [10] for $k=0,1,...,18$). In turn, these values of p_k yield the following large q expansions of $\bar{R}(q)$ and $\bar{c}(q)$

$$\boxed{\begin{aligned}
\bar{R}(q) &= q+1+\frac{2}{q}+\frac{2}{q^2}+\frac{2}{q^3}-\frac{4}{q^5}-\frac{8}{q^6}-\frac{12}{q^7}-\frac{10}{q^8}-\frac{4}{q^9}+\frac{12}{q^{10}}+\frac{46}{q^{11}} \\
&+\frac{98}{q^{12}}+\frac{154}{q^{13}}+\frac{124}{q^{14}}+\frac{10}{q^{15}}-\frac{102}{q^{16}}+\frac{20}{q^{17}}-\frac{64}{q^{18}}+O(\frac{1}{q^{19}}) \\
\bar{c}(q) &= 1-\frac{1}{q}-\frac{4}{q^2}-\frac{4}{q^3}+\frac{14}{q^5}+\frac{44}{q^6}+\frac{56}{q^7}+\frac{28}{q^8}-\frac{82}{q^9}-\frac{252}{q^{10}}-\frac{388}{q^{11}} \\
&-\frac{588}{q^{12}}-\frac{772}{q^{13}}-\frac{620}{q^{14}}+\frac{1494}{q^{15}}+\frac{5788}{q^{16}}+\frac{7580}{q^{17}}-\frac{690}{q^{18}}+O(\frac{1}{q^{19}})
\end{aligned}} \tag{4.14}$$

Moreover, due to the intrinsic polynomial character of the large q expansion (4.13), we find that

$$\boxed{\gamma(q) = 0} \tag{4.15}$$

This result is expected to hold as long as the corrections to the polynomial behavior of the $\bar{M}_n^{(n-k)}$ are negligible. This condition defines precisely the large q phase $q > q_c$. Therefore the exponent $\gamma(q)$ vanishes identically over the whole phase $q > q_c$.

It is interesting to compare the result of these large q expansions to the previous direct large n extrapolations. As far as $\bar{R}(q)$ is concerned, we find a perfect agreement for the values $q \geq 2$, down to $q = 2$, where we find $\bar{R}(2) \simeq 4.442(1)$ using (4.14), in perfect agreement with the previous estimate. The precision of (4.14) increases with q, leading to far better estimates than before: $\bar{R}(3) \simeq 4.92908(1)$, $\bar{R}(4) \simeq 5.6495213(1)$...

As to $\gamma(q)$, our prediction that $\gamma(q) = 0$ for all $q > 2$ is compatible with the previous extrapolation of Fig.20, where this value is represented in dashed line (indeed, the large q expansions give precise results down to $q \sim 2$ where the extrapolations become dubious). We therefore expect $\gamma(q)$ to have a discontinuity at $q = 2$, where it goes from a non-zero $\gamma(q = 2^-)$ value to zero.

This is further confirmed by a refined analysis of the average winding (2.2) in the large q phase. This requires a refined study of the semi-meander numbers $\bar{M}_n^{(n-k)}(w)$ with fixed winding w, which display a similar polynomial structure as the $\bar{M}_n^{(n-k)}$. As a result, we find that

$$\boxed{\langle w \rangle_n(q) \;=\; \lambda(q) n + \mu(q)} \tag{4.16}$$

hence $\nu(q) = 1$ throughout the large q phase, and the coefficients $\lambda(q)$ and $\mu(q)$ have the following large q expansions up to order 14 in $1/q$

$$\boxed{\begin{aligned}
\lambda(q) \;&=\; 1 - \frac{2}{q} - \frac{2}{q^2} + \frac{2}{q^3} + \frac{2}{q^4} + \frac{2}{q^5} + \frac{10}{q^6} - \frac{6}{q^7} - \frac{14}{q^8} - \frac{10}{q^9} \\
&\quad + \frac{22}{q^{10}} + \frac{86}{q^{11}} - \frac{58}{q^{12}} - \frac{222}{q^{13}} - \frac{118}{q^{14}} + O(\frac{1}{q^{15}}) \\
\mu(q) \;&=\; \frac{2}{q} + \frac{10}{q^2} + \frac{22}{q^3} + \frac{54}{q^4} + \frac{134}{q^5} + \frac{246}{q^6} + \frac{622}{q^7} + \frac{1434}{q^8} + \frac{3178}{q^9} \\
&\quad + \frac{6834}{q^{10}} + \frac{13786}{q^{11}} + \frac{30834}{q^{12}} + \frac{66590}{q^{13}} + \frac{140582}{q^{14}} + O(\frac{1}{q^{15}})
\end{aligned}} \tag{4.17}$$

The plot of the function $\lambda(q)$ is displayed in Fig.22. Remarkably, this coefficient seems to vanish at the point $q = 2$ with an excellent precision. Since this coefficient must be positive, we deduce that our large q formulas break down for $q < 2$. We interpret this as

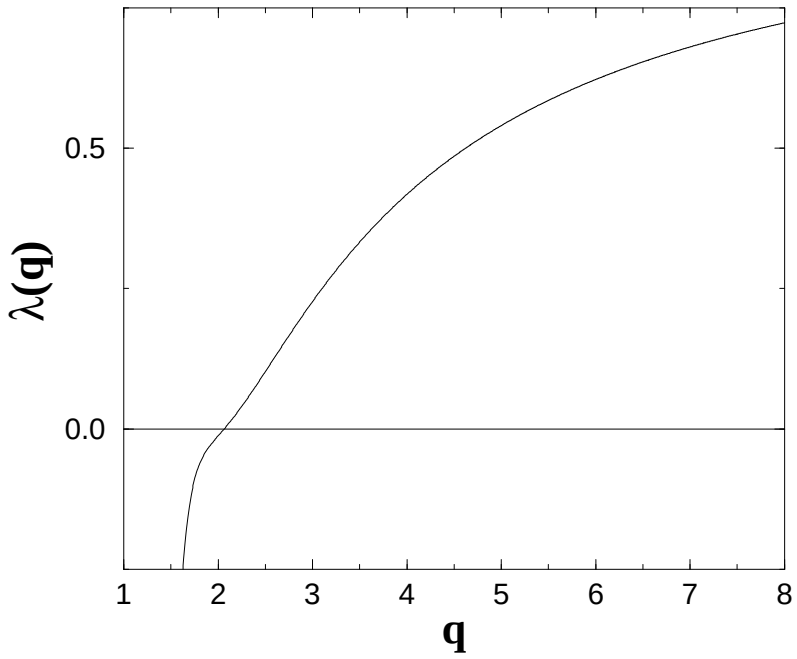

Fig. 22: The series $\lambda(q)$ (4.17) of $1/q$ up to order 14, for $1 < q < 8$. The curve seems to vanish precisely at $q = 2$.

yet another evidence of the drastic change of behavior of the average winding $\langle w \rangle$, which is no longer linear in n below q_c, and we find $q_c = 2$ with an excellent precision.

In conclusion, we gave strong evidence for the existence of a winding transition of the semi-meander partition function in the large n limit, taking place at a value $q_c = 2$ which we conjecture to be exact. The order parameter for this transition is clearly

$$\boxed{\lim_{n\to\infty} \frac{1}{n}\langle w \rangle_n \;=\; \begin{cases} \lambda(q) & \text{for } \; q > q_c \\ 0 & \text{for } \; q < q_c \end{cases}} \tag{4.18}$$

which vanishes for $q < q_c$ (irrelevant winding, i.e. $\nu(q) < 1$) and is nonzero for $q > q_c$ (relevant winding, i.e. $\nu(q) = 1$). With the order parameter (4.18), the transition is found to be continuous, as the leading coefficient $\lambda(q)$ (4.17) vanishes at $q = q_c$. As argued before, The low-q phase is characterized by a meander-type behavior of the semi-meander polynomial, where $\bar{R}(q) = R(q)$. The smooth character of the transition is also visible from the fact that $\bar{R}(q)$ approaches $R(q)$ tangentially at $q = q_c$ (c.f. Fig.18).

5. Conclusion

We must admit that none of the compact expressions (matrix model and symmetric group) for the meander and semi-meander numbers, although conceptually interesting

(beautiful?), give an efficient way of computing them. There is always some lengthy process involved, such as evaluating Gaussian averages of traces of words or writing the group characters, which render the evaluation in fact untractable. The Temperley-Lieb algebra connection is maybe one of the most promising approaches towards exact asymptotics, but we have no definite answer to this day.

In the direct enumerative approach, we have analyzed the meander problem in the language of critical phenomena, by analogy with Self-Avoiding Walks. In particular, we have displayed various scaling behaviors, involving both scaling exponents and scaling functions. We have presented strong evidence for the existence of a phase transition for semi-meanders weighed by a factor q per connected component (road).

In a large-q regime ($q > q_c$), the winding is found to be relevant, with a winding exponent $\nu(q) = 1$, while the configuration exponent $\gamma(q) = 0$. In this regime, the partition function per bridge for semi-meanders $\bar{R}(q)$ is strictly larger than that of meanders $R(q)$. The particular form of its large q series expansion in $1/q$ (4.14) with slowly alternating integer coefficients, which furthermore grow very slowly with the order, suggests a possible re-expression in terms of modular forms of q, yet to be found. It is striking to notice that our numerical estimate for $\bar{R}(2)$ agrees up to the third digit with the value

$$\pi\sqrt{2} \;=\; 4\prod_{k=1}^{\infty}\frac{(4k)^2}{(4k+1)(4k-1)} \;=\; 4.4428... \tag{5.1}$$

suggesting maybe an infinite product form for $\bar{R}(q)$, which is still to be found.

In a low-q regime $q < q_c$, $\bar{R}(q)$ and $R(q)$ coincide, in agreement with an irrelevant winding $\nu(q) < 1$. The exponent $\gamma(q)$ is no longer 0, but a strictly positive function of q. We have estimated the value of the transition point $q_c \simeq 2$ with an excellent precision, and we conjecture that $q_c = 2$ exactly. This special value of q has actually been singled out in the algebraic study of the meander problem, in connection with the Temperley-Lieb algebra as sketched in Sect.3.3. Indeed, as shown in [9], one can re-express the meander and semi-meander partition functions as that of some Restricted Solid-On-Solid model, whose Boltzmann weights are positive precisely iff $q \geq 2$, indicating very different behaviors for $q < 2$ and $q > 2$.

There still remains to find the varying exponents $\gamma(q)$ and $\nu(q)$ in the $q < 2$ regime, as well as the precise value of $R(q) = \bar{R}(q)$. Although we improved our numerical estimates, we are limited to conjectures. For $q = 0$, we confirm a previous conjecture [7] that $\gamma = 2$, and that [6] $\alpha = 7/2$. We also conclude from the numerical analysis that $\nu(0) \simeq 0.52(1)$ is definitely not equal to the trivial random-walk exponent $1/2$.

References

[1] K. Hoffman, K. Mehlhorn, P. Rosenstiehl and R. Tarjan, *Sorting Jordan sequences in linear time using level-linked search trees*, Information and Control **68** (1986) 170-184.

[2] V. Arnold, *The branched covering of $CP_2 \to S_4$, hyperbolicity and projective topology*, Siberian Math. Jour. **29** (1988) 717-726.

[3] K.H. Ko, L. Smolinsky, *A combinatorial matrix in 3-manifold theory*, Pacific. J. Math **149** (1991) 319-336.

[4] J. Touchard, *Contributions à l'étude du problème des timbres poste*, Canad. J. Math. **2** (1950) 385-398.

[5] W. Lunnon, *A map–folding problem*, Math. of Computation **22** (1968) 193-199.

[6] S. Lando and A. Zvonkin, *Plane and Projective Meanders*, Theor. Comp. Science **117** (1993) 227-241, and *Meanders*, Selecta Math. Sov. **11** (1992) 117-144.

[7] P. Di Francesco, O. Golinelli and E. Guitter, *Meander, folding and arch statistics*, to appear in Journal of Mathematical and Computer Modelling (1996).

[8] Y. Makeenko, *Strings, Matrix Models and Meanders*, proceedings of the 29th Inter. Ahrenshoop Symp., Germany (1995); Y. Makeenko and H. Win Pe, *Supersymmetric matrix models and the meander problem*, preprint ITEP-TH-13/95 (1996); G. Semenoff and R. Szabo *Fermionic Matrix Models* preprint UBC/S96/2 (1996).

[9] P. Di Francesco, O. Golinelli and E. Guitter, *Meanders and the Temperley-Lieb algebra*, Saclay preprint T96/008 (1996).

[10] P. Di Francesco, O. Golinelli and E. Guitter, *Meanders: a direct enumeration approach*, Saclay preprint T96/062 (1996).

[11] H. Temperley and E. Lieb, *Relations between the percolation and coloring problem and other graph-theoretical problems associated with regular planar lattices: some exact results for the percolation problem*, Proc. Roy. **A322** (1971) 251-280.

[12] N. Sloane, *The on–line encyclopedia of integer sequences*, e-mail: sequences@research.att.com

[13] R. Baxter, *Exactly solved models in statistical mechanics*, Academic Press, London (1982).

[14] E. Brézin, C. Itzykson, G. Parisi and J.-B. Zuber, *Planar Diagrams*, Commun. Math. Phys. **59** (1978) 35-51; P. Di Francesco, P. Ginsparg and J. Zinn-Justin *2D Gravity and Random Matrices*, Phys. Rep. **254** (1995) 1-133.

[15] P. Martin, *Potts models and related problems in statistical mechanics*, World Scientific (1991).